Exosomes derived from EphB2-overexpressing bone marrow mesenchymal stem cells regulate immune balance and repair barrier function

Si Chu
Huazhong University of Science and Technology Tongji Medical College
Ting Yu
Huazhong University of Science and Technology Tongji Medical College
Wenzhu Wang
Huazhong University of Science and Technology Tongji Medical College
Hui Wu
Huazhong University of Science and Technology Tongji Medical College
Feng Zhu
Huazhong University of Science and Technology Tongji Medical College
Chunzhu Wei
Huazhong University of Science and Technology Tongji Medical College
Fei Gao
Huazhong University of Science and Technology Tongji Medical College
Chang Liu
Huazhong University of Science and Technology Tongji Medical College
Heng Fan (cs19940307@sina.com)
Huazhong University of Science and Technology Tongji Medical College https://orcid.org/0000-0001-6639-3474

Research Article

Keywords: Exosome, bone marrow mesenchymal stem cell, EphB2, T cell differentiation, intestinal barrier function, Caco-2 cell

Posted Date: September 21st, 2022

DOI: https://doi.org/10.21203/rs.3.rs-2040313/v1

Version of Record: A version of this preprint was published at Biotechnology Letters on April 10th, 2023. See the published version at https://doi.org/10.1007/s10529-023-03358-y.

Abstract

Background

Disruption of intestinal barrier function and an imbalance in intestinal immunity are crucial for the occurrence and development of ulcerative colitis. Because of their important roles in regulating inflammation and immunity, exosomes (Exos) released from bone marrow mesenchymal stem cells (BMSCs) may be useful for treating ulcerative colitis. The EphB/EphrinB signaling pathway plays a crucial role in the inflammatory process and the development and function of immune cells, and can mediate long-distance intercellular communication through extracellular vesicles. This study was conducted to explore the effects of pre-modified BMSC-Exos expressing EphB2 (EphB2-Exos) on immunoregulation *in vitro.*

Methods

We transfected a lentivirus vector encoding EphB2 into BMSCs and isolated EphB2-Exos from the culture supernatant. Inflammation and oxidative damage in the human colon adenocarcinoma cell line (Caco-2) were induced by dextran sulfate sodium/hydrogen peroxide. In addition, spleen $CD4^+$ T lymphocytes of rats were sorted *in vitro*. We conducted a series of experiments to explore the biological functions of EphB2-Exos.

Results

EphB2-Exos were successfully isolated and were found to significantly protect the activity, proliferation, and migration of Caco-2 cells that were inhibited by dextran sulfate sodium. EphB2-Exos alleviated inflammation and apoptosis and increased the activity of antioxidant enzymes while inhibiting oxidative stress in Caco-2 cells. EphB2-Exos restored barrier function by inhibiting the RhoA/ROCK pathway and regulated the polarization of $CD4^+$T cells.

Conclusion

EphB2-Exos enhanced intestinal barrier function and regulated the immune balance by inhibiting the RhoA/ROCK pathway *in vitro*. These findings suggest that EphB2-Exos can be applied as a cell-free therapy for ulcerative colitis.

1. Introduction

Ulcerative colitis (UC) is an inflammatory bowel disease that is often accompanied by alternating episodes and remissions. In recent years, the global incidence of UC has increased annually. However,

existing therapeutic drugs cannot completely cure the disease and exhibit some side effects and drug resistance [1, 2]. Therefore, new drugs must be developed. The pathogenesis of UC has been traditionally thought to involve genetics, environmental factors, immune disorders, and intestinal microbes; however, the precise mechanism underlying the pathogenesis of this disease remains unclear. Recently, through the accelerated pace of research, the innate immune system and its interaction with gut microbes and the adaptive immune system have been shown to be important factors in UC [2].

Exosomes are extracellular vesicles with a double-layer membrane structure that are derived from a wide range of sources; they are typically 30–150 nm in diameter and can carry nucleic acids, proteins, and other biologically active ingredients [3]. Bone marrow mesenchymal stem cells (BMSCs) are a type of pluripotent stem cells that reside with hematopoietic stem cells in the bone marrow cavity and exhibit multi-differentiation abilities. Initially, these cells were used as therapeutic tools to treat bone and cartilage diseases. According to recent studies, BMSCs can home to the injured site by producing bioactive ingredients and anti-inflammatory factors, reducing inflammation at the injured site and promoting the repair and regeneration of damaged tissues [4–6]. Other recent studies have demonstrated that exosomes released from BMSCs (BMSC-Exos) can increase the production of anti-inflammatory factors, inhibit inflammatory responses, and regulate immunity. BMSC-Exos have been shown to reduce the expression of the pro-inflammatory cytokines, interleukin-1 beta (IL-1β) and tumor necrosis factor-alpha, and increase the expression of anti-inflammatory cytokine transforming growth factor β (TGF-β) in *in vitro* studies. In addition, BMSC-Exos regulate the proliferation and transformation of T cells, promote the transformation of Th1 cells into Th2 cells, and reduce the production of Th17 cells [7, 8]. As a cell-free therapy, exosomes are safer and more stable than BMSCs. Based on these advantages, exosomes may be useful for treating inflammatory bowel disease (IBD).

Culture conditions, such as genetic modification, can enhance the functions of mesenchymal stem cells (MSCs) *in vivo* and *in vitro* [9]. Pre-treated MSCs show better paracrine function and homing ability to the injured site than untreated MSCs [10, 11]. Recent studies have demonstrated that in experimental colitis mice, MSCs treated with IL-1β exhibit an increased ability to migrate to the spleen, mesenteric lymph nodes, and colon, and there is a low proportion of M1 macrophages in the abdominal cavity of the mice [11, 12]. Erythropoietin-producing hepatocellular (Eph) receptors form the largest family of receptor tyrosine kinases, and bidirectional signal transduction between Eph and its ligand Ephrin activates bidirectional communication between the receptor and ligand cells [13–16]. The Eph-Ephrin axis can control cell migration [17–19]. Recent studies have revealed that intestinal epithelial cells 6 cultured *in* vitro show high expression of EphrinB1 and EphrinB2 ligands, and during intestinal repair, their reverse signals can regulate inflammation and accelerate intestinal injury repair [20]. Eph/ephrin molecules have been reported to be involved in the development and function of immune cells [21]. EphrinB1, which is highly expressed by human primary T cells, shows high affinity with EphB2, which is highly expressed by MSCs [22]. Previous studies have found that EphrinB1/EphB2 reverse signaling inhibits the proliferation of mouse T cells [23]. However, the effect of the EphB2/EphrinB1 axis on BMSCs-Exos and its potential role in UC immune regulation *in vitro* have not been reported previously.

In the present study, we aimed to investigate the effect of BMSCs-Exos pretreated with lentivirus overexpressing EphB2 on the biological function of Caco-2 cells exposed to dextran sodium sulfate (DSS) or H_2O_2. We also evaluated the modulatory effect of EphB2-Exos on the polarization of Th1, Th17, and regulatory T (Treg) cells *in vitro*.

2. Materials And Methods

2.1. BMSC isolation, expansion, and identification

All animals used in this study were purchased from Hubei Bente Biotechnology Co., Ltd. (Wuhan, China). The entire research process was supported and supervised by the Animal Care and Use Committee of Tongji Medical College, Huazhong University of Science and Technology, China. BMSCs were isolated from male Sprague Dawley rats weighing 60–100 g according to previously described methods [24, 25]. Briefly, the bone marrow in the rat femur and tibia flushed out using a 5-mL sterile syringe was cultured in DMEM/F12 (Gibco, Grand Island, NY, USA) containing 10% exosome-depleted fetal bovine serum (Gibco, Australia) in a humidified atmosphere of 5% CO_2. After culturing the cells for 48 h, the medium was changed to remove non-adherent cells. When the cells reached 80–90% confluence, they were digested with trypsin (0.05% Trypsin-EDTA, Gibco, Canada) and then subcultured and expanded. At passages 3–5 (P3–P5), the cells were labeled with antibodies against CD29, CD90, CD45, and CD11b (BioLegend, San Diego, CA, USA), and BMSCs were phenotyped by flow cytometry.

2.2. Construction of recombinant lentivirus carrying EphB2

We used GenBank to design forward (5'-GTCAACACGCTGGACAAGAT-3') and reverse (5'-CCTTATAGTCCTTATCATCGTC-3') primers, which were synthesized by Shanghai Generay Biotech Co., Ltd. (Shanghai, China). After the amplified EphB2 gene fragment was inserted into the lentiviral vector GV342 (Ubi-MCS-SV40-puromycin), the linearized GV342 vector was used to amplify the EphB2 gene fragment using polymerase chain reaction (PCR). Positive clones with 394-bp PCR products were selected for sequencing. This recombinant lentivirus was designed with both the puromycin-resistant gc green fluorescent protein gene. After co-transfection with GV492 and packaging plasmids, pHelper 1.0 and pHelper 2.0 (Genechem), recombinant lentivirus was produced by 293T cells.

2.3. Lentiviral transfection of BMSCs

P2–P3 BMSCs were inoculated into the culture flask and cultured for approximately 8–12 h until reaching 30–40% confluence, following which transfection was performed at a multiplicity of infection of 30–35 using an appropriate dose of HitransG P, according to the manufacturer's instructions. The genetically engineered BMSCs used recombinant lentiviruses that simultaneously expressed EphB2 and puromycin-resistant genes. The negative control used an empty lentivirus with anti-puromycin gene but not the EphB2 gene. Approximately 48–72 h after transfection, the medium containing lentivirus was discarded and replaced with complete medium. To screen for the stable expression of EphB2-BMSCs, puromycin was added to the complete medium to a final concentration of 2–3 mg/mL, and the medium

was changed daily for 7 days. The obtained stably transfected cells were expanded to generations P4–P5 and used for exosome extraction.

2.4. Exosome isolation, purification, and identification

To prepare the exosomes, we cultured P4–P5 BMSCs to approximately 80–90% confluence and then cultured the cells in serum-free DMEM/F12 for 48 h to obtain more exosomes, following which the cell culture supernatants were collected. Exosomes were acquired by ultracentrifugation, first by centrifuging the cell culture supernatant at 300 ×*g* for 15 min and then at 2000 ×*g* for 30 min. The obtained supernatant was centrifuged at 12,000 ×*g* for 30 min. To remove excess cell debris, the supernatant was filtered through a 0.22-μm filter. The supernatants were ultra-centrifuged twice (Beckman, Brea, CA, USA) at 120,000 ×*g* for 90 min, which yielded the pure exosomes. All the above steps were conducted at 4°C (Fig. 1).

To demonstrate the successful isolation of exosomes, the morphology of the enriched exosomes was observed using transmission electron microscopy (TEM) (Tecnai, FEI, Hillsboro, OR, USA). The marker proteins on exosomes (CD9, CD63, and TSG101) were detected by western blotting. The size distribution of exosomes was measured using nanoparticle tracking analysis (NanoSight, Salisbury, UK). After quantifying the protein concentration of exosomes using a BCA kit (Beyotime Biotechnology, China), the exosomes were stored at -80°C until analysis.

2.5. Cell culture

Caco-2 cells were purchased from Shanghai Zhong Qiao Xin Zhou Biotechnology Co. (Shanghai, China) and cultured in high-glucose (HG)-DMEM (Gibco, Waltham, MA, USA) containing 10% FBS, 2.5% HEPES (Sigma, St. Louis, MO, USA), and 1% antibiotics (Sigma-Aldrich, St Louis, MO, USA) and seeded onto culture flasks (25 or 75 cm^2). The complete medium was replaced every two days; when the cells were 90% confluent, they were digested with 0.25% trypsin-EDTA for cell subculture. This cell line is commonly used in studies of intestinal epithelial wound healing [26].

2.6. CCK-8 assay

The effect of EphB2-Exos on the viability of Caco-2 cells was evaluated in a Cell Counting Kit-8 (CCK-8, Dojindo, Kumamoto, Japan) assay. After Caco-2 cells were seeded onto 96-well plates and cultured for 12 h, the complete medium was replaced with HG-DMEM containing 2% serum, and exosomes and EphB2-Exos were added to the medium. After 24 h of treatment, CCK-8 reagent with a final concentration of 10% was added to the 96-well plate. After incubation for 2 h at 37°C, the amount of formazan formed was detected by measuring the absorbance at 450 nm with a reference wavelength of 655 nm using a multimode plate reader (PerkinElmer EnSpire Plate Reader, Waltham, MA, USA).

2.7. Wound-healing assay

Caco-2 cells were seeded onto a six-well plate at a density of 3×10^5 cells per well. After the cells reached around 90% confluence, scratch analysis was performed. The scratches in each well were created using a

sterile 10-μL pipette tip. The scraped floating cells were washed twice with PBS, and the remaining cells were incubated with EphB2-Exos. An optical microscope (Olympus, Tokyo, Japan) was used to photograph the same locations along the scratch wound at 0 and 24 h. ImageJ software 8.0 (NIH, Bethesda, MD, USA) was used to measure the areas of the scratch wounds.

2.8. Induction of oxidative stress in Caco-2 cells

The culture medium of Caco-2 cells grown in six-well plates was collected to detect peroxides and antioxidant enzymes. The cells were pretreated with exosomes and EphB2-Exos for 12 h. To mimic oxidative damage, in addition to the control group, 250 μM hydrogen peroxide (H_2O_2, Sigma-Aldrich, St. Louis, MO) was added to the Caco-2 cells in each group. The experimental groups were as follows: (1) control, (2) H_2O_2 (250 μmol/L), (3) exosomes (30 μg/mL), and (4) EphB2-Exos (30 μg/mL). After treatment for 24 h, the cells were collected and used to detect the concentrations of myeloperoxidase (MPO), superoxide dismutase (SOD), glutathione (GSH), malondialdehyde (MDA), and nitric oxide (NO) using a commercial assay kit (Nanjing Jiancheng, China), and the cell culture media from each group were collected for subsequent experiments.

2.9. Measurement of intracellular reactive oxygen species levels

The reactive oxygen species (ROS) generation test was performed as previously described [27]. For the experiment, 3×10^5 Caco-2 cells per well were seeded into a 6-well black plate in complete culture medium. The groups of cells were prepared and treated as described previously. After these steps, the medium was aspirated, and cells were washed twice with PBS. Next, 1 mL of 2',7'-dichlorofluorescein diacetate (DCFH-DA) was added to each well at a concentration of 10 μM, and the cells were further incubated at 37°C under 5% CO_2 for 60 min. After incubation, DCFH-DA was removed, and the cells were washed with PBS. The negative controls contained cells in DMEM, whereas positive controls contained cells in DMEM with 20 μM hydrogen donor for 60 min. The medium was aspirated, and the cells were collected with PBS. These suspensions were centrifuged at 300 ×*g* for 5 min; the pellet was washed twice with PBS and then suspended in sterile PBS. The fluorescence of the cells was assessed by flow cytometry. The average 2',7'-dichlorofluorescein (DCF) fluorescence was determined as a percentage compared to the negative control, which was assumed to be 100%.

2.10. Enzyme-linked immunosorbent assay

Cell culture medium samples were obtained from the different groups, and the protein levels of IL-1β, IL-6, IL-17A, IL-10, and TGF-β1 in the media were measured using enzyme-linked immunosorbent assay kits (Elabscience Biotechnology Co., Ltd., Houston, TX, USA) according to the manufacturer's instructions.

2.11. Fluorescein isothiocyanate-dextran permeability assay

To measure intestinal barrier function, we seeded 5×10^4 Caco-2 cells onto the apical side of 24-well Transwell polyester membrane filters (6.5 mm diameter, 3 μm pore size; Corning, Inc., Corning, NY, USA) and cultured the cells for at least 21 days. Cells in the upper chamber were pretreated with exosomes or EphB2-Exos for 24 h, and 3% DSS dissolved in DMEM was added to the upper chamber for 8 h. To determine the permeability of cell monolayers, the cells were incubated with fluorescein isothiocyanate-dextran (FD-4, 4 kDa, 1 mg/mL; Sigma-Aldrich, St. Louis, MO) in the upper chamber for 2 h at 37°C; subsequently, 100 μL of samples from the outer chamber was collected for assessment using a multimode plate reader at excitation and emission wavelengths of 485 and 535 nm, respectively. The dextran concentration in each sample was calculated using a fluorescein isothiocyanate-dextran standard curve.

2.12. Western blotting

Caco-2 cell proteins were extracted using RIPA lysis solution containing a cocktail of protease inhibitors (Servicebio Technology, Wuhan, China). After treatment, the Caco-2 cells were washed twice with cold PBS, and RIPA lysis solution was added to the cells. The protein concentration was determined using a BCA protein assay kit (Beyotime Biotechnology, China). The same mass of protein was separated using 8–12% sodium dodecyl sulfate–polyacrylamide gel electrophoresis and transferred onto polyvinylidene fluoride membranes (Millipore, Billerica, MA, USA). After blocking with 5% skimmed milk, the membranes were incubated with primary antibodies against EphB2 (1:500; Abcam, Cambridge, UK), EphrinB1 (1:500; Cell Signaling Technology Inc., Danvers, MA, USA), RhoA (1:2000; Abcam), ROCK1 (1:2000; Abcam), ROCK2 (1:2000; Abcam), occludin (1:1000; Abcam), ZO-1 (1:2000; Abcam) and β-actin (1:10,000; CST) overnight at 4°C. Next, the membranes were washed three times with PBS containing Tween 20 and incubated with the appropriate secondary antibody at 25°C for 1 h. Finally, the membranes were visualized according to the manufacturer's instructions.

2.13. Isolation and culture of CD4 $^{+}$ *T lymphocytes*

CD4^{+}T lymphocytes were isolated from the fresh spleens of male rats weighing 80 g using a CD4^{+} negative isolation kit (Stem Cell Technologies, Vancouver, BC, Canada) according to the manufacturer's instructions. The cells were cultured in 96-well flat bottom plates (2×10^5 cells/well) in RPMI-1640 (Gibco, Eggenstein, Germany) containing 10% fetal bovine serum, 1% antibiotics (penicillin –streptomycin), 1% sodium pyruvate, and 1% Glutamax (Invitrogen, Burlington, ON, Canada).

2.13. Co-culture of EphB2-Exos and CD4 $^{+}$ *T lymphocytes*

The effect of EphB2-Exos on CD4^{+} T lymphocytes *in vitro* was investigated by co-culturing CD4^{+} T lymphocytes and exosomes. A 96-well flat-bottomed plate was pre-coated with anti-CD3 antibody (5 μg/mL, BD Biosciences, Franklin Lakes, NJ, USA) and anti-CD28 antibody (10 μg/mL, BD Biosciences) overnight at 4°C to activate the CD4^{+} T lymphocytes. Subsequently, CD4^{+} T lymphocytes were added to the plate, which was washed twice with PBS. After 4 h, exosomes or EphB2-Exos were added, whereas CD4^{+} T lymphocytes were untreated (negative controls). The cells were maintained at 37°C for 3 days in a humidified incubator with 5% CO_2. After 72 h of incubation, the CD4^{+} T lymphocytes were stained with PE-Cy7-anti-CD4 antibody (BD Biosciences), eFluor450-anti-IL-17A antibody (eBioscience, San Diego, CA, USA), PE-anti-Foxp3 antibody

(eBioscience), or APC-anti-IFN-γ antibody (BD Biosciences). The stained cells were analyzed using flow cytometry.

2.14. Statistical analyses

All experimental data are presented as the mean ± standard error of the mean. Comparisons between multiple groups were evaluated using one-way analysis of variance followed by Tukey's post hoc test. Statistical analysis was performed using GraphPad Prism (GraphPad Prism 8.4.2, USA). $P < 0.05$ was considered statistically significant.

3. Results

3.1. Characterization of BMSCs and exosomes

BMSCs were purified from Sprague Dawley rat bone marrow tissue and characterized based on their morphological properties and immunophenotypes at passage 3. Spindle-shaped BMSCs exhibited plastic adhesion and formed swirling colonies (Fig. 2A). The purity of the BMSCs was evaluated by flow cytometry analysis of specific cell surface markers. As illustrated in Fig. 2B, BMSCs highly expressed CD29 and CD90 but expressed minimal levels of CD11b and CD45. The former are surface markers of hematopoietic cells, whereas the latter are surface markers for bone marrow progenitor cells. The extracted exosomes were characterized using TEM, nanoparticle tracking analysis, and western blotting. TEM images showed that most exosomes were within 200 nm in diameter and had a cup- or round-shaped morphology (Fig. 2C). The diameter of the exosomes was approximately 85 nm (Fig. 2E). The expression of TSG101, CD63, and CD9 proteins was detected by western blot analysis (Fig. 2D). Collectively, these data confirmed the successful isolation of exosomes from BMSCs.

3.2. Expression of EphB2 was upregulated in BMSCs and exosomes after lentivirus intervention

We successfully constructed a lentivirus carrying the EphB2 gene and obtained BMSCs stably overexpressing EphB2 by *in vitro* transduction with lentivirus and puromycin screening. EphB2-BMSCs with gcGFP gene were observed to emit green fluorescence under a fluorescence microscope at 72 hours of lentivirus transfection (Fig. 2F). The corresponding reverse transcription-PCR results were obtained from our previous study [28]. The expression of EphB2 was upregulated successfully in BMSCs and exosomes after lentivirus intervention compared to the negative groups.

3.3. EphB2-Exos promote the viability and migration of Caco-2 cells

To explore the influence of EphB2-Exos on the viability and migration of Caco-2 cells (Fig. 3A), we defined 4 groups (control, DSS, exosome, and EphB2-Exos groups). The viability of Caco-2 cells treated with EphB2-Exos was measured using the CCK-8 assay, which showed that DSS inhibited the activity of Caco-2 cells, whereas exosomes protected against this effect, and the protective effect of EphB2-Exos was stronger (Fig. 3B). To explore the effect of EphB2-Exos on injury repair *in vitro*, we conducted a wound-healing assay. DSS inhibited damage repair, whereas exosomes promoted wound healing; among the treatments, EphB2-Exos exhibited the strongest protective effect (Fig. 3C, D). These results indicate that EphB2-Exos rescued the viability of Caco-2 cells inhibited by DSS and promoted wound healing.

3.4. EphB2-Exos inhibit oxidative stress in Caco-2 cells

In this experiment, to explore whether EphB2-Exos could affect the oxidative stress of Caco-2 cells, we exposed the cells to H_2O_2 and constructed an oxidative damage model of Caco-2 cells. The enzyme activities of superoxide dismutase and glutathione in the cell lysate and supernatant were significantly decreased in the H_2O_2 group. The malondialdehyde and myeloperoxidase levels in the cell lysate or supernatant increased after adding H_2O_2. The protective effect of superoxide dismutase against glutathione was observed in cells treated with exosomes, particularly in the EphB2-Exos group (Fig. 4A). These results indicated that EphB2-Exos alleviated the oxidative stress response of Caco-2 cells caused by H_2O_2.

3.5. Measurement of intracellular ROS production

As ROS production is common in every cell line and is typically involved in inflammatory conditions, we analyzed redox signaling by measuring ROS production. We observed significant increases in ROS levels in Caco-2 cells. Intracellular ROS levels were analyzed using the fluorescent probe 6-carboxy 2',7'-dichlorodihydrofluorescein diacetate (carboxy-H2DCFDA). Carboxy-H2DCFDA diffuses into cells and is hydrolyzed to DCFH. DCFH trapped within the cells is converted to DCF by ROS-mediated oxidation. The H_2O_2 group exhibited a higher level of ROS than the control group. Although the exosomes significantly reduced ROS production compared to H_2O_2, the effect of EphB2-Exos was stronger (Fig. 4B). These results suggested that antioxidant enzyme activities are upregulated in Caco-2 cells.

3.6. EphB2-Exos alleviate inflammatory responses in Caco-2 cells

The concentrations of pro- and anti-inflammatory cytokines in Caco-2 cells were determined using commercially available enzyme-linked immunosorbent assay kits. The protein expression of pro-inflammatory cytokines, including IL-1β, IL-6, and IL-17A, was significantly elevated after 8 h of incubation with DSS; however, the protein levels of IL-10 and TGF-β1 were downregulated (Fig. 4C). The

exosomes prevented increases in the levels of the above-mentioned pro-inflammatory cytokines. Exosomes upregulated IL-10 and TGF-β1 protein levels. Compared with exosomes, EphB2-Exos exhibited a similar but more powerful regulatory effect.

3.7. EphB2-Exos improve intestinal permeability in Caco-2 cells

FD-4 cannot pass through a complete intestinal barrier; however, FD-4 can penetrate the blood through an injured or damaged intestine. In this study, intestinal barrier function was assessed indirectly through intestinal permeability analysis. DSS disrupted the Caco-2 cell monolayer, resulting in a significant increase in the level of FD-4 in the medium, and these increases were reversed when exosomes were added. In addition, EphB2-Exos significantly reduced the levels of FD-4 in the medium (Fig. 5A).

In addition, the protein expression of ZO-1 and occludin in Caco-2 cells decreased after DSS intervention, whereas exosomes reversed this effect (Fig. 5B). These results suggest that exosomes can ameliorate DSS-induced epithelial barrier damage; this effect was more pronounced when EphB2-Exos were used.

3.8. EphB2-Exos enhance ZO-1 and occludin expression by inhibiting the RhoA-ROCK signaling pathway

To explore whether EphB2-Exos improves intestinal permeability by regulating the tight junction protein, the expression of ZO-1 and occludin in Caco-2 cells was measured by western blotting. After DSS treatment, the expression levels of ZO-1 and occludin proteins decreased, and exosomes reversed this change (Fig. 5B). The RhoA-ROCK signaling pathway is involved in regulating T cell activation and intestinal barrier damage [29, 30]. Therefore, we analyzed the protein expression of RhoA, ROCK1, and ROCK2. ROCK1 and ROCK2 protein levels increased after DSS intervention in Caco-2 cells and decreased significantly after treatment with EphB2-Exos (Fig. 6A, B). Activation of the RhoA/ROCK signaling pathway was significantly induced after DSS incubation, and EphB2-Exos significantly inhibited the activation of this signaling pathway. These results suggest that EphB2-Exos enhance the expression of ZO-1 and occludin by inhibiting the RhoA/ROCK signaling pathway.

3.9. Effect of EphB2-Exos on the polarization of Th1, Th17, and Treg cells in vitro

To determine the effect of EphB2-Exos on the polarization of $CD4^+$ T cells, rat spleen $CD4^+$ T lymphocytes were obtained by magnetic bead sorting (Fig. 7A). After 72 h of stimulation with exosomes and EphB2-Exos and corresponding cytokines (Fig. 7A), we assessed the proportion of Th1, Th17, and Treg cells among all $CD4^+$ T cells. After treatment with the exosomes, the proportions of $CD4^+IFN\text{-}\gamma^+$ Th1 cells and $CD4^+IL17A^+$ Th17 cells were significantly decreased (Fig. 7B, C); in contrast, the proportion of $CD4^+Foxp3^+$ Treg cells increased (Fig. 7D). After EphB2-Exos treatment, each subgroup showed the same change as the exosome group; however, the change was more exaggerated. These results indicate that

EphB2-Exos inhibited $CD4^+$ T lymphocyte differentiation into Th1 and Th17 cells but induced them to differentiate into Treg cells *in vitro* (Fig. 7E–G).

4. Discussion

We found that EphB2-Exos effectively reversed the inhibitory effects of DSS on Caco-2 cell viability and migration. *In vitro* experiments showed that EphB2-Exos alleviated the inflammatory response and oxidative stress of Caco-2 cells and enhanced intestinal barrier repair by inhibiting the RhoA-ROCK pathway. Additionally, EphB2-Exos were found to regulate the polarization of Th1, Th17, and Treg cells *in vitro*. These findings highlight that EphB2-Exos can relieve intestinal inflammation, repair the intestinal barrier, and restore intestinal immune balance, demonstrating the potential of EphB2-Exos for treating UC.

Innate immunity (mainly impaired intestinal barrier and microbial interaction) and adaptive immune disorders have been generally thought to play an essential role in the occurrence and development of UC [2, 31]. Intestinal barrier damage leads to increased intestinal permeability, which may result from regulatory defects of tight junction proteins. Intestinal epithelial cells have the basic function as a physical barrier, in addition to producing antimicrobial peptides and other substances to build defenses and prevent the invasion of bacteria and other microorganisms [32–34]. Studies have shown that patients with IBD are characterized by intestinal epithelial barrier damage and dysfunction, and healthy family members of these patients also have intestinal epithelial barrier dysfunction without IBD, suggesting that these factors cause IBD [35, 36]. We previously showed that EphB2-EVs can alleviate intestinal inflammation in rats with DSS-induced experimental colitis and increase the expression of intestinal tight junction proteins [28]. In this study, we demonstrated that EphB2-Exos can enhance the function of Caco-2 cells, improve intestinal permeability, and promote barrier repair.

Recent studies have focused on modifying exosomes to enhance their therapeutic effects. Eph/ephrin molecules participate in many important physiological activities in the body, including embryogenesis, inflammation regulation, and blood vessel formation. In addition, they regulate the adhesion and migration of MSCs. Wnt/β-catenin and its downstream EphB/EphrinB signal transduction are key to the proliferation and localization of intestinal epithelial cells during migration [37]. After the intestinal epithelium is damaged, rapid recovery of the intestinal surface is highly dependent on the ability of epithelial cells on the edge of the damage to rapidly form pseudopodia, reorganize the cytoskeleton, and quickly migrate to the damaged site [38, 39]. To protect the host from several pathogenic microorganisms and exposure to various intestinal pathogens and toxic factors, the rapid healing ability of the intestinal epithelium is particularly important [39]. Recent studies have shown that EphB/ephrinB signaling plays a key role in the repair and maintenance of intestinal tissues [37]. In the present study, we administered EphB2-Exos to Caco-2 cells treated with DSS. ZO-1 and occludin protein expression indicated that EphB2-Exos promoted the expression of tight junction proteins and repaired the intestinal tract. In addition, FD-4 analysis showed that DSS destroyed the permeability of the cell monolayer; EphB2-Exos reversed this effect, indirectly indicating that EphB2-Exos can enhance intestinal permeability and repair the intestinal epithelial barrier.

RhoA is a small GTPase in the Rho family and is involved in several cellular processes, including cell proliferation and differentiation. Rho-related kinases (ROCK), including ROCK1 and ROCK2, have been identified as key effectors of RhoA, which regulates various physiological functions through the phosphorylation of downstream targets such as MYPT-1, MLC, and ERM. The signaling pathway mediated by Rho GTPase plays an important role in regulating the immune response mediated by T cells, including the development, activation, and differentiation of T cells. Recently, studies have found that ROCK activity is elevated in various autoimmune diseases, including systemic lupus erythematosus, rheumatoid arthritis, and idiopathic pulmonary fibrosis. In addition, an increase in RhoA-ROCK related pathway protein levels has been observed in the intestinal mucosa of patients with active CD [41]. In mice and humans with arthritis, ROCK2 has been shown to upregulate IL-17A and IL-21 expression in CD4 + T cells by phosphorylating IRF and Stat3 [40]. ZO-1 and occludin are essential proteins for maintaining the permeability of the intestinal epithelial barrier, and Rho kinase regulates tight junctions, specifically occludin. Owing to the action of DSS, the cells release numerous inflammatory factors; the Ras homolog (Rho) protein is activated, and it binds to ROCK. The activated RhoA/ROCK signaling pathway regulates polymerization of the actin cytoskeleton, thereby increasing the distance between intestinal epithelial cells and regulating intestinal permeability [41, 42]. Our results showed that DSS treatment leads to decreased levels of the tight junction proteins, ZO-1 and occludin, in Caco-2 cells and increased levels of RhoA, ROCK1, and ROCK2; following EphB2-Exos treatment, the levels of tight junction proteins decreased. After this reversal, the levels of constituent proteins in the RhoA/ROCK signaling pathway decreased. These findings indicate that the RhoA/ROCK signal transduction is involved in repairing the intestinal epithelial barrier by EphB2-Exos.

A common feature of patients with IBD is the infiltration of inflammatory CD4 + T cells. Among these cells, the main pro-inflammatory cells are Th1 and Th17; their infiltration is accompanied by a lack of immunosuppressive T cells, such as Treg cells that express Foxp3 [43–45]. EphB/ephrin B signaling has an important influence on the development of the thymus and T-cell proliferation. We found that mice lacking the EphB2 gene showed insufficient thymic lymphocytes and decreased cell migration. The bidirectional conduction between EphB/ephrin-B is essential for MSC-mediated suppression of activated T cells [22]. In previous studies, we investigated the effect of EphB2-EVs on Th17 and Treg cells in the spleen and mesenteric lymph nodes of experimental colitis rats. Here, we examined the effect of EphB2-Exos on the polarization of Th1, Th17, and Treg cells *in vitro* by isolating $CD4^+$ T lymphocytes from the rat spleen. The results indicate that EphB2-Exos effectively prevent the differentiation of $CD4^+$ T cells into Th1 and Th17 cells and significantly increase the proportion of Treg cells in $CD4^+$ T cells. Additionally, these data demonstrate that EphB2-Exos can regulate the balance between Th1 and Th17/Treg cells. The present study provides new evidence regarding the effect of EphB2-Exos on improving intestinal barrier dysfunction and regulating intestinal immune balance. It additionally indicates the potential of a new treatment strategy for UC and other immune-related diseases.

5. Conclusions

In conclusion, exosomes released from EphB2-BMSCs enhanced the viability of Caco-2 cells and promoted their proliferation and migration, thereby promoting barrier repair and regulating T cell polarization (Fig. 8). Intestinal barrier repair was achieved by inhibiting the RhoA/ROCK pathway. However, further research is needed to explore whether EphB2-Exos regulate T cell balance *in vitro* through the RhoA/ROCK pathway. We demonstrate a promising alternative strategy for treating UC and other immunological diseases.

Declarations

Declarations of interest

None.

Acknowledgements

The authors thank Dr Chengcheng Yin for helpful discussion.

Funding

This study was supported by the National Natural Science Foundation of China (81774093).

Author contributions

S.C. and H.F. conceived and designed the study. S.C., T.Y., W.W., H.W., X.L., F.Z., C.W., F.G. and C.L. performed the experiments. S.C., T.Y. and H.F. analyzed the data. S.C., T.Y., and W.W. wrote the manuscript. All authors read and approved the final manuscript.

References

1. Renna S, Cottone M, Orlando A (2014) Optimization of the treatment with immunosuppressants and biologics in inflammatory bowel disease. World J Gastroenterol 20:9675–9690. https://doi:10.3748/wjg.v20.i29.9675
2. Kaser A, Zeissig S, Blumberg RS (2010) Inflammatory bowel disease. Annu Rev Immunol 28:573–621. https://doi:10.1146/annurev-immunol-030409-101225
3. Zhang H, Wang L, Li C, Yu Y, Yi Y, Wang J, Chen D (2019) Exosome-Induced Regulation in Inflammatory Bowel Disease. Front Immunol 10:1464. https://doi:10.3389/fimmu.2019.01464
4. Hofstetter CP, Schwarz EJ, Hess D, Widenfalk J, El Manira A, Prockop DJ, Olson L (2002) Marrow stromal cells form guiding strands in the injured spinal cord and promote recovery. Proc Natl Acad Sci U S A 99:2199–2204. https://doi:10.1073/pnas.042678299
5. González MA, Gonzalez-Rey E, Rico L, Büscher D, Delgado M (2009) Adipose-derived mesenchymal stem cells alleviate experimental colitis by inhibiting inflammatory and autoimmune responses. Gastroenterology 136:978–989. https://doi:10.1053/j.gastro.2008.11.041

6. Jurewicz M, Yang S, Augello A, Godwin JG, Moore RF, Azzi J, Fiorina P, Atkinson M, Sayegh MH, Abdi R (2010) Congenic mesenchymal stem cell therapy reverses hyperglycemia in experimental type 1 diabetes. Diabetes 59:3139–3147. https://doi:10.2337/db10-0542
7. Chen W, Huang Y, Han J, Yu L, Li Y, Lu Z, Li H, Liu Z, Shi C, Duan F et al (2016) Immunomodulatory effects of mesenchymal stromal cells-derived exosome. Immunol Res 64:831–840. https://doi:10.1007/s12026-016-8798-6
8. Harrell CR, Jovicic N, Djonov V, Arsenijevic N and Volarevic V. Mesenchymal Stem Cell-Derived Exosomes and Other Extracellular Vesicles as New Remedies in the Therapy of Inflammatory Diseases. Cells 2019;8. https://doi:10.3390/cells8121605
9. Hu C, Li L (2018) Preconditioning influences mesenchymal stem cell properties in vitro and in vivo. J Cell Mol Med 22:1428–1442. https://doi:10.1111/jcmm.13492
10. François M, Romieu-Mourez R, Li M, Galipeau J (2012) Human MSC suppression correlates with cytokine induction of indoleamine 2,3-dioxygenase and bystander M2 macrophage differentiation. Mol Ther 20:187–195. https://doi:10.1038/mt.2011.189
11. Carrero R, Cerrada I, Lledó E, Dopazo J, García-García F, Rubio MP, Trigueros C, Dorronsoro A, Ruiz-Sauri A, Montero JA et al (2012) IL1β induces mesenchymal stem cells migration and leucocyte chemotaxis through NF-κB. Stem Cell Rev Rep 8:905–916. https://doi:10.1007/s12015-012-9364-9
12. Fan H, Zhao G, Liu L, Liu F, Gong W, Liu X, Yang L, Wang J, Hou Y (2012) Pre-treatment with IL-1β enhances the efficacy of MSC transplantation in DSS-induced colitis. Cell Mol Immunol 9:473–481. https://doi:10.1038/cmi.2012.40
13. Lisabeth EM, Falivelli G, Pasquale EB (2013) Eph receptor signaling and ephrins. Cold Spring Harb Perspect Biol 5. https://doi:10.1101/cshperspect.a009159
14. Pasquale EB (2010) Eph receptors and ephrins in cancer: bidirectional signalling and beyond. Nat Rev Cancer 10:165–180. https://doi:10.1038/nrc2806
15. Pasquale EB (2008) Eph-ephrin bidirectional signaling in physiology and disease. Cell 133:38–52. https://doi:10.1016/j.cell.2008.03.011
16. Kullander K, Klein R (2002) Mechanisms and functions of Eph and ephrin signalling. Nat Rev Mol Cell Biol 3:475–486. https://doi:10.1038/nrm856
17. Barquilla A, Pasquale EB (2015) Eph receptors and ephrins: therapeutic opportunities. Annu Rev Pharmacol Toxicol 55:465–487. https://doi:10.1146/annurev-pharmtox-011112-140226
18. Cho HJ, Hwang YS, Yoon J, Lee M, Lee HG, Daar IO (2018) EphrinB1 promotes cancer cell migration and invasion through the interaction with RhoGDI1. Oncogene 37:861–872. https://doi:10.1038/onc.2017.386
19. Himanen JP, Saha N, Nikolov DB (2007) Cell-cell signaling via Eph receptors and ephrins. Curr Opin Cell Biol 19:534–542. https://doi:10.1016/j.ceb.2007.08.004
20. Hafner C, Meyer S, Hagen I, Becker B, Roesch A, Landthaler M, Vogt T (2005) Ephrin-B reverse signaling induces expression of wound healing associated genes in IEC-6 intestinal epithelial cells. World J Gastroenterol 11:4511–4518. https://doi:10.3748/wjg.v11.i29.4511

21. Wu J, Luo H (2005) Recent advances on T-cell regulation by receptor tyrosine kinases. Curr Opin Hematol 12:292–297. https://doi:10.1097/01.moh.0000166497.26397.9f
22. Nguyen TM, Arthur A, Hayball JD, Gronthos S (2013) EphB and Ephrin-B interactions mediate human mesenchymal stem cell suppression of activated T-cells. Stem Cells Dev 22:2751–2764. https://doi:10.1089/scd.2012.0676
23. Kawano H, Katayama Y, Minagawa K, Shimoyama M, Henkemeyer M, Matsui T (2012) A novel feedback mechanism by Ephrin-B1/B2 in T-cell activation involves a concentration-dependent switch from costimulation to inhibition. Eur J Immunol 42:1562–1572. https://doi:10.1002/eji.201142175
24. Zhang L, Jiao G, Ren S, Zhang X, Li C, Wu W, Wang H, Liu H, Zhou H, Chen Y (2020) Exosomes from bone marrow mesenchymal stem cells enhance fracture healing through the promotion of osteogenesis and angiogenesis in a rat model of nonunion. Stem Cell Res Ther 11:38. https://doi:10.1186/s13287-020-1562-9
25. Xu R, Zhang F, Chai R, Zhou W, Hu M, Liu B, Chen X, Liu M, Xu Q, Liu N et al (2019) Exosomes derived from pro-inflammatory bone marrow-derived mesenchymal stem cells reduce inflammation and myocardial injury via mediating macrophage polarization. J Cell Mol Med 23:7617–7631. https://doi:10.1111/jcmm.14635
26. Charrier L, Yan Y, Driss A, Laboisse CL, Sitaraman SV, Merlin D (2005) ADAM-15 inhibits wound healing in human intestinal epithelial cell monolayers. Am J Physiol Gastrointest Liver Physiol 288:G346–353. https://doi:10.1152/ajpgi.00262.2004
27. Hu L, Wang H, Huang L, Zhao Y, Wang J (2016) The Protective Roles of ROS-Mediated Mitophagy on (125)I Seeds Radiation Induced Cell Death in HCT116 Cells. Oxid Med Cell Longev 2016:9460462. https://doi:10.1155/2016/9460462
28. Yu T, Chu S, Liu X, Li J, Chen Q, Xu M, Wu H, Li M, Dong Y, Zhu F et al (2021) Extracellular vesicles derived from EphB2-overexpressing bone marrow mesenchymal stem cells ameliorate DSS-induced colitis by modulating immune balance. Stem Cell Res Ther 12:181. https://doi:10.1186/s13287-021-02232-w
29. Bros M, Haas K, Moll L, Grabbe S RhoA as a Key Regulator of Innate and Adaptive Immunity. Cells 2019;8. https://doi:10.3390/cells8070733
30. Zhao H, Sun X, Tong J (2020) Role of ROCK/NFkappaB/AQP8 signaling in ethanolinduced intestinal epithelial barrier dysfunction. Mol Med Rep 22:2253–2262. https://doi:10.3892/mmr.2020.11318
31. Geremia A, Biancheri P, Allan P, Corazza GR, Di Sabatino A (2014) Innate and adaptive immunity in inflammatory bowel disease. Autoimmun Rev 13:3–10. https://doi:10.1016/j.autrev.2013.06.004
32. Mehandru S, Colombel JF (2021) The intestinal barrier, an arbitrator turned provocateur in IBD. Nat Rev Gastroenterol Hepatol 18:83–84. https://doi:10.1038/s41575-020-00399-w
33. Vancamelbeke M, Vermeire S (2017) The intestinal barrier: a fundamental role in health and disease. Expert Rev Gastroenterol Hepatol 11:821–834. https://doi:10.1080/17474124.2017.1343143
34. Odenwald MA, Turner JR (2017) The intestinal epithelial barrier: a therapeutic target? Nat Rev Gastroenterol Hepatol 14:9–21. https://doi:10.1038/nrgastro.2016.169

35. May GR, Sutherland LR, Meddings JB (1993) Is small intestinal permeability really increased in relatives of patients with Crohn's disease? Gastroenterology 104:1627–1632. https://doi:10.1016/0016-5085(93)90638-s
36. Katz KD, Hollander D, Vadheim CM, McElree C, Delahunty T, Dadufalza VD, Krugliak P, Rotter JI (1989) Intestinal permeability in patients with Crohn's disease and their healthy relatives. Gastroenterology 97:927–931. https://doi:10.1016/0016-5085(89)91499-6
37. Batlle E, Henderson JT, Beghtel H, van den Born MM, Sancho E, Huls G, Meeldijk J, Robertson J, van de Wetering M, Pawson T et al (2002) Beta-catenin and TCF mediate cell positioning in the intestinal epithelium by controlling the expression of EphB/ephrinB. Cell 111:251–263. https://doi:10.1016/s0092-8674(02)01015-2
38. Jacinto A, Martinez-Arias A, Martin P (2001) Mechanisms of epithelial fusion and repair. Nat Cell Biol 3:E117–123. https://doi:10.1038/35074643
39. Wilson AJ, Gibson PR (1997) Epithelial migration in the colon: filling in the gaps. Clin Sci (Lond) 93:97–108. https://doi:10.1042/cs0930097
40. Yoseph BP, Klingensmith NJ, Liang Z, Breed ER, Burd EM, Mittal R, Dominguez JA, Petrie B, Ford ML, Coopersmith CM (2016) Mechanisms of Intestinal Barrier Dysfunction in Sepsis. Shock 46:52–59. https://doi:10.1097/SHK.0000000000000565
41. Jin Y, Blikslager AT (2020) The Regulation of Intestinal Mucosal Barrier by Myosin Light Chain Kinase/Rho Kinases. Int J Mol Sci 21. https://doi:10.3390/ijms21103550
42. Wang Y, Wang X, Yang W, Zhao X, Zhang R (2018) Effect of Simvastatin on the Intestinal Rho/ROCK Signaling Pathway in Rats With Sepsis. J Surg Res 232:531–538. https://doi:10.1016/j.jss.2018.07.016
43. Tindemans I, Joosse ME, Samsom JN Dissecting the Heterogeneity in T-Cell Mediated Inflammation in IBD. Cells 2020;9. https://doi:10.3390/cells9010110
44. Liu H, Dasgupta S, Fu Y, Bailey B, Roy C, Lightcap E, Faustin B (2019) Subsets of mononuclear phagocytes are enriched in the inflamed colons of patients with IBD. BMC Immunol 20:42. https://doi:10.1186/s12865-019-0322-z
45. Rovedatti L, Kudo T, Biancheri P, Sarra M, Knowles CH, Rampton DS, Corazza GR, Monteleone G, Di Sabatino A, Macdonald TT (2009) Differential regulation of interleukin 17 and interferon gamma production in inflammatory bowel disease. Gut 58:1629–1636. https://doi:10.1136/gut.2009.182170

Figures

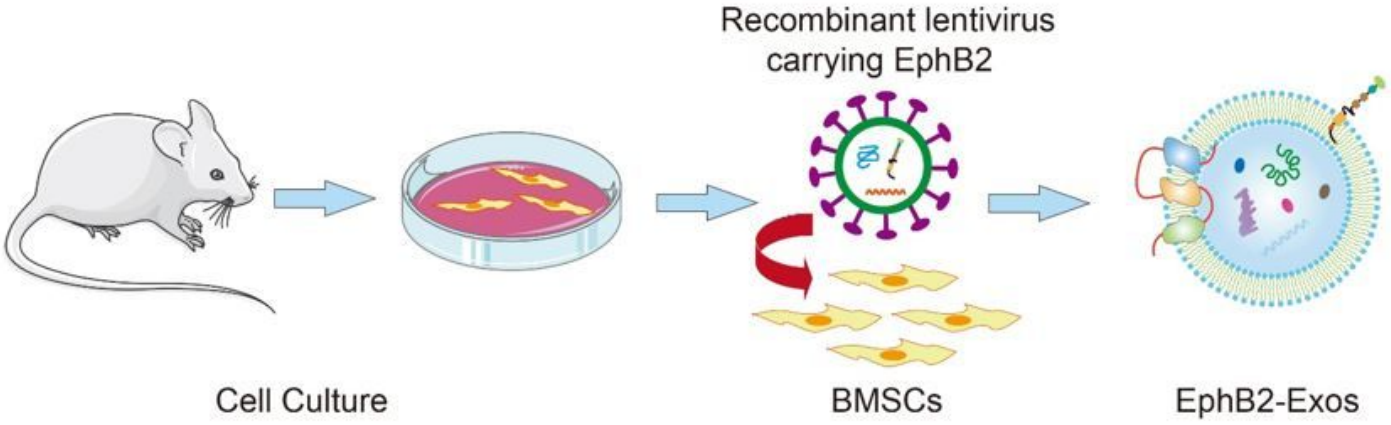

Figure 1

Extraction of exosomes from BMSCs carrying overexpressing EphB2 lentivirus.

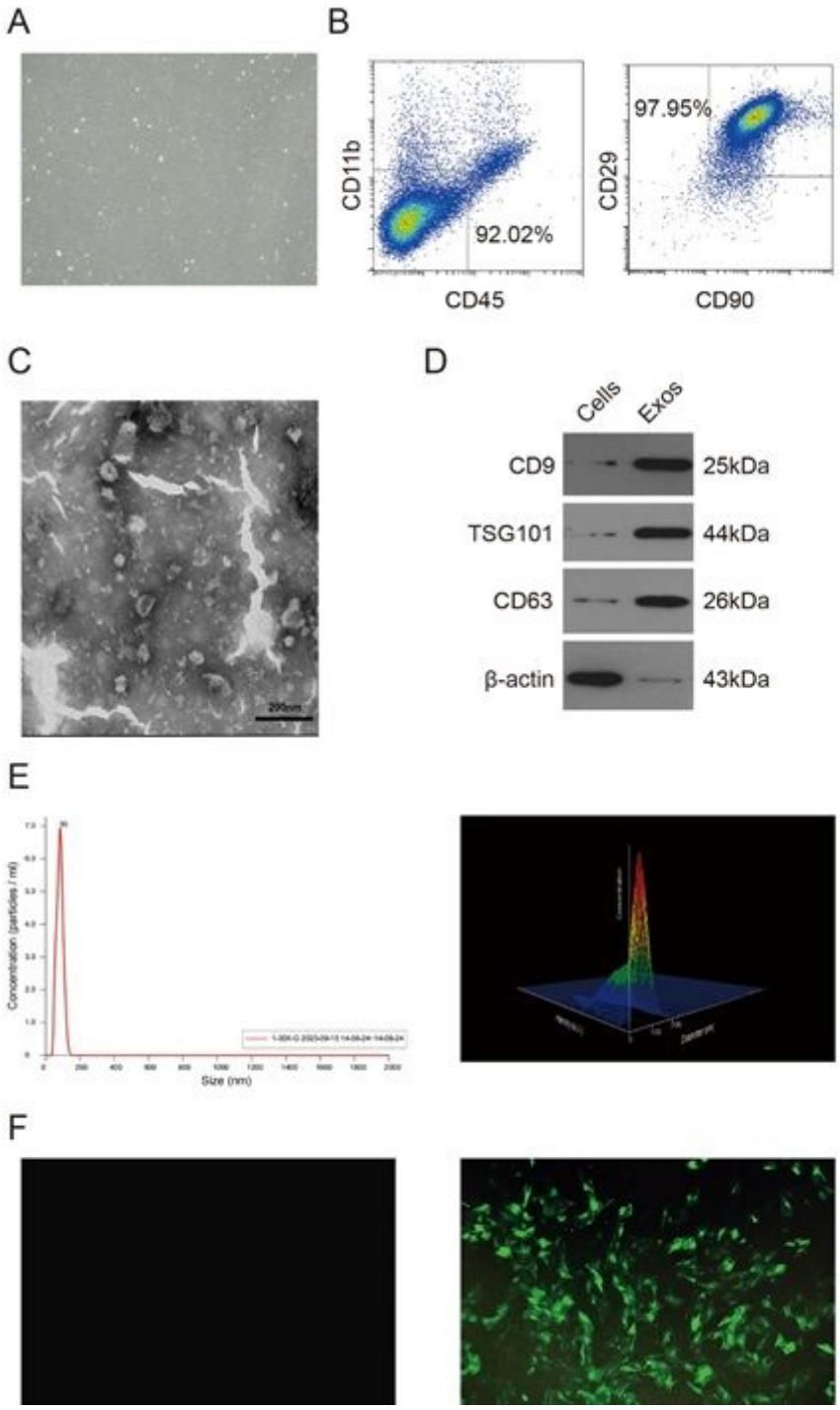

Figure 2

Characterization of EphB2-BMSCs and EphB2-Exos. (A) The morphological image of P3 BMSCs (Original magnification, × 40). (B) Flow cytometric identification of characteristic markers of BMSCs. (C) The morphology of EphB2-Exos under transmission electron microscopy (Scale bar = 200 nm). (D) Western blotting analysis of EphB2-Exos marker proteins CD9, CD63 and TSG101. (E) The size distribution of EphB2-Exos by NTA. (F) Fluorescence microscopy imaging of null-BMSCs and EphB2-BMSCs with GFP (Original magnification, × 100).

3.2. Expression of EphB2 was upregulated in BMSCs and exosomes after lentivirus intervention

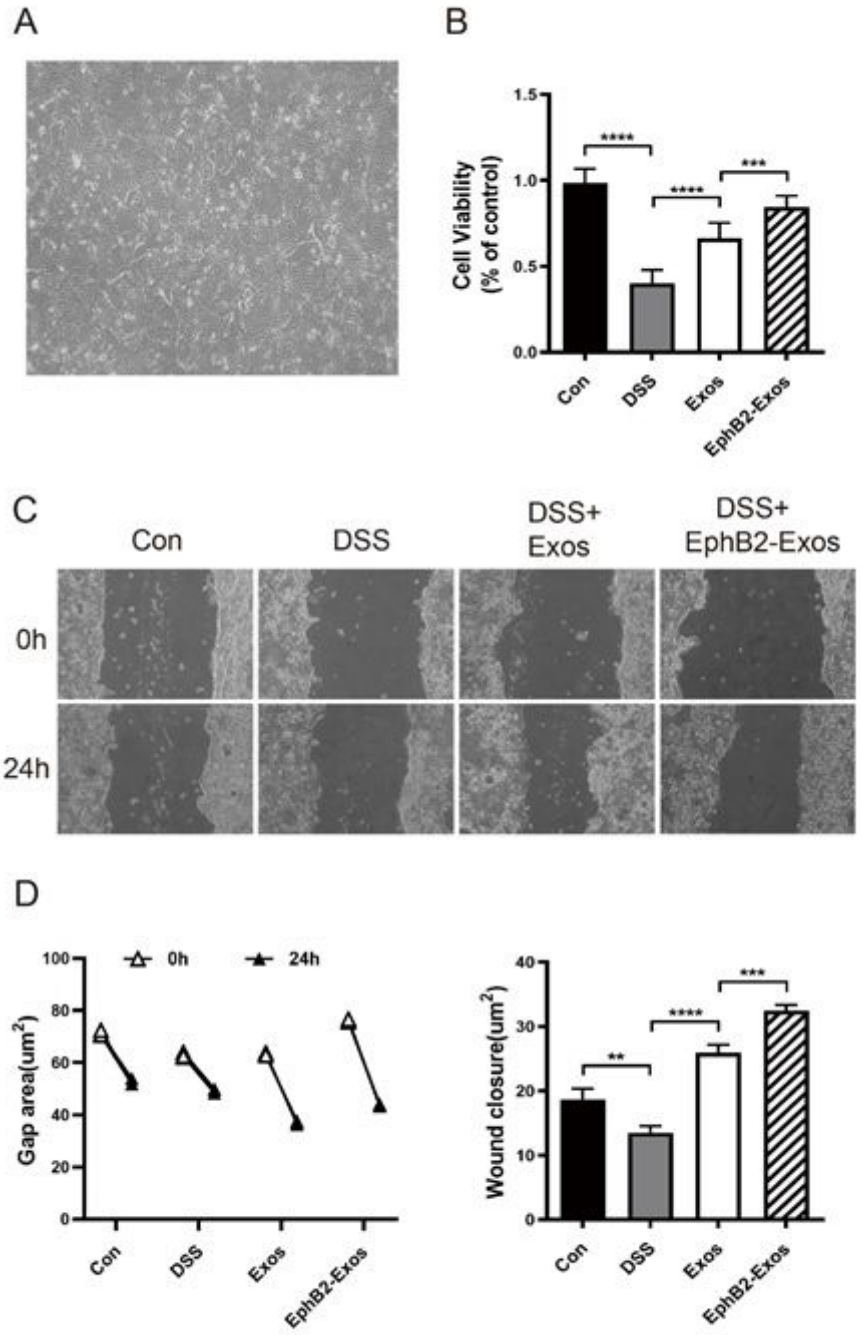

Figure 3

EphB2-Exos enhanced the viability and migration of Caco-2 cells. (A) The morphological image of Caco-2 cells observed under optical microscope (Original magnification, × 40). (B) CCK8 assay was performed to evaluate Caco-2 cells viability after treatment with DSS and EphB2-Exos. The cell viability was normalized to control group. (C) Wound healing assay of the Caco-2 cells. (D) Quantitative analysis of gap areas and wound closure in Caco-2 cells. Statistical analysis performed using one-way ANOVA with a Tukey Kramer post-hoc test. **P 0.01, ***P 0.001, ****P 0.0001.

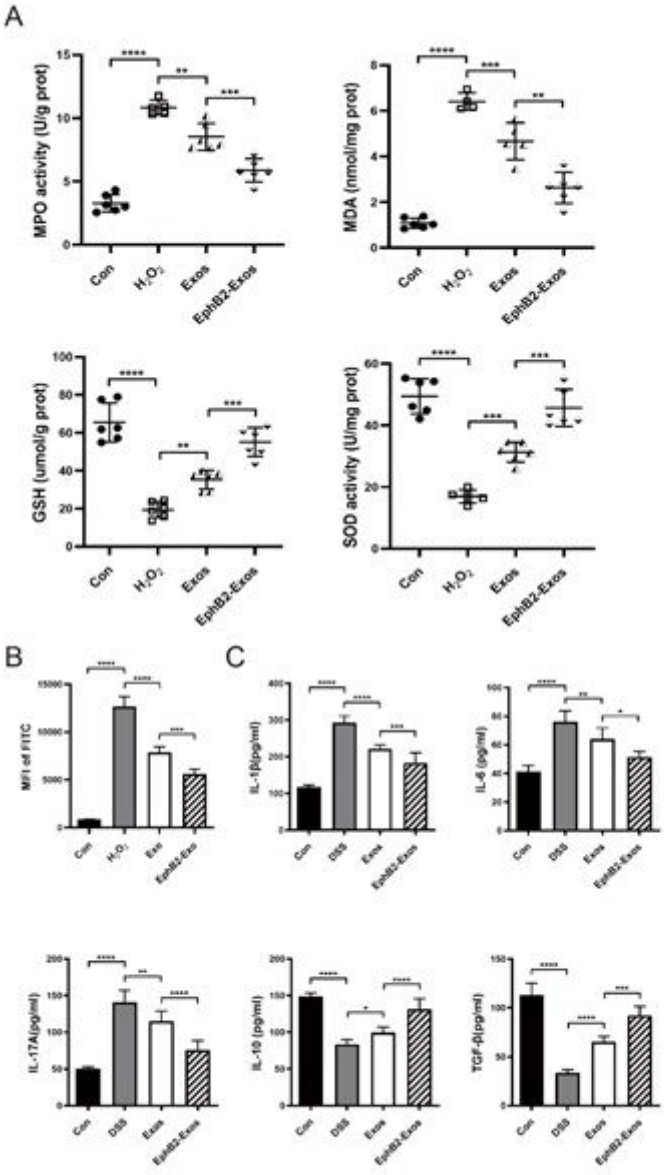

Figure 4

EphB2-Exos alleviated inflammation and oxidative stress in Caco-2 cells. (A) Expression levels of MPO, MDA, GSH, and SOD in Caco-2 cells after treatment with H2O2and EphB2-Exos. (B) Caco-2 cells exposed to H2O2 were treated with EphB2-Exos for 12 hours. The intracellular ROS production was detected with ROS assay kit. DCFH-DA was added to Caco-2 cells and left for 60 min fluorescence of oxidized DCF was followed by emission and excitation wavelengths of 535 nm and 485 nm, respectively. (C) Protein levels of IL-1β, IL-6, IL-17A, IL-10 and TGF-β in Caco-2 cells from the four groups by ELISA. Statistical analysis performed using one-way ANOVA with a Tukey Kramer post-hoc test. *P 0.05, **P 0.01, ***P 0.001, ****P 0.0001.

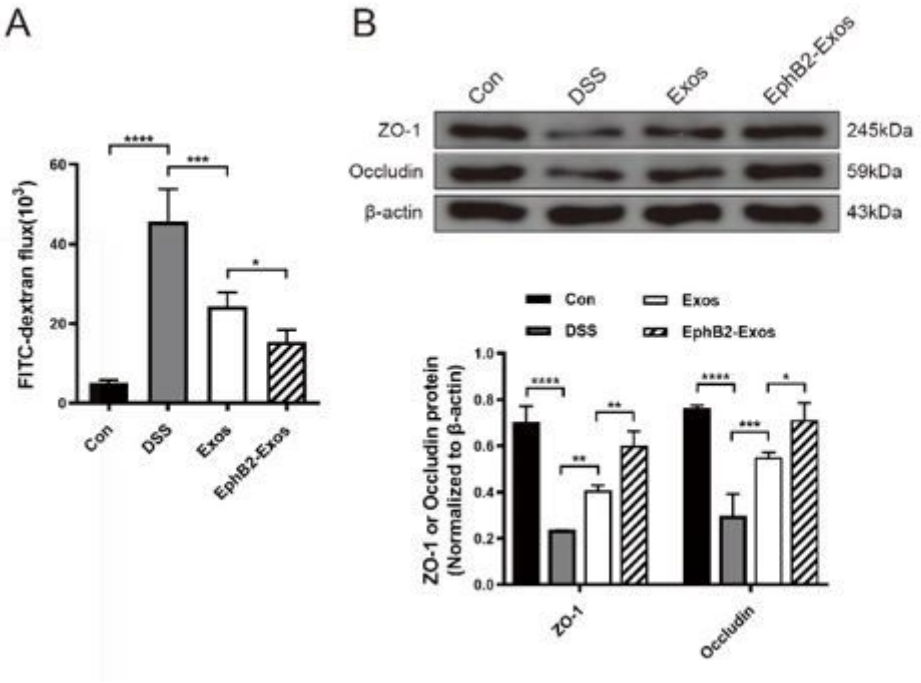

Figure 5

EphB2-Exos promoted repairment of barrier dysfunction induced by DSS. (A) Cumulative FD-4 leakage in 2 h after EphB2-Exos treated DSS-induced barrier dysfunction in the transwell co-culture model. (B) The protein expression of TJ proteins ZO-1 and occludin in Caco-2 cells. The protein expression was normalized to β-actin. Statistical analysis performed using one-way ANOVA with a Tukey Kramer post-hoc test. *P 0.05, **P 0.01, ***P 0.001, ****P 0.0001.

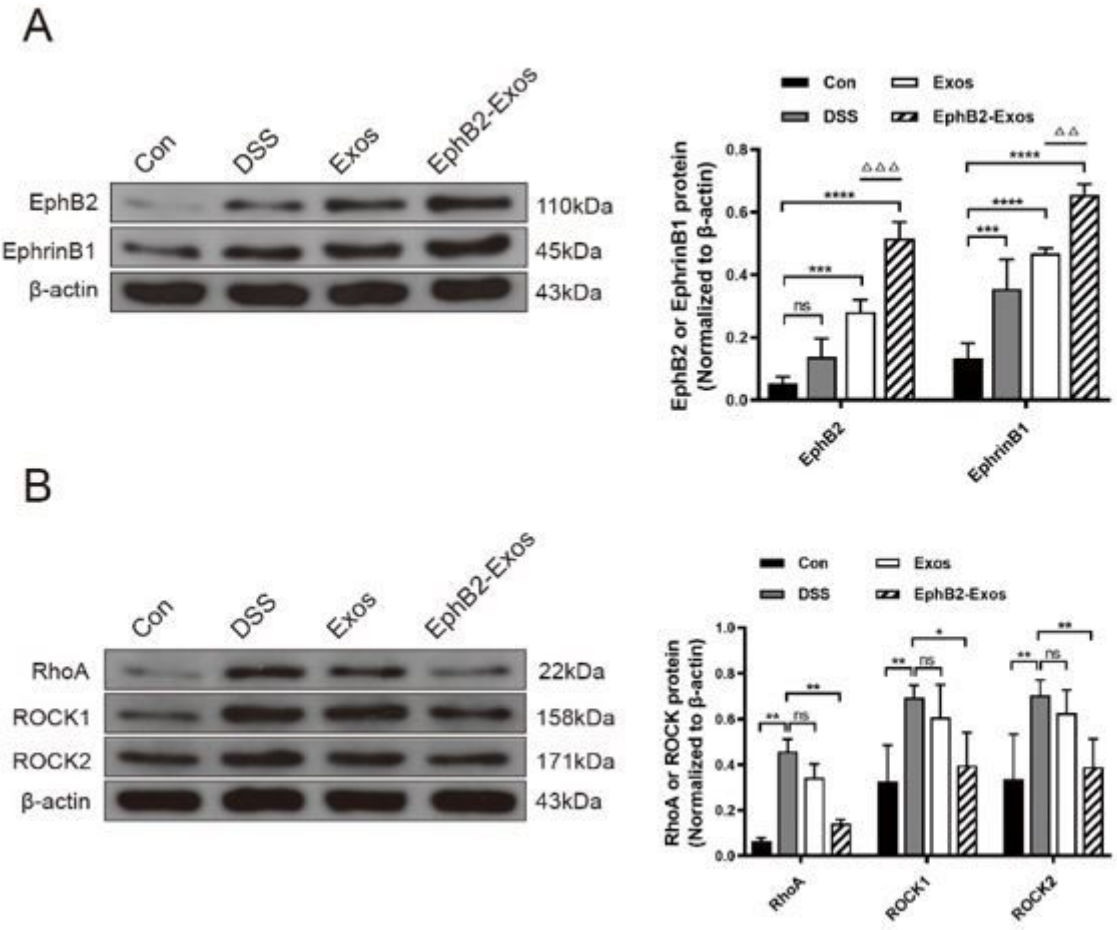

Figure 6

EphB2-Exos inhibited RhoA/ROCK pathway in Caco-2 cells. (A) Western blotting analysis of EphB2 and ephrin-B1 proteins and quantitative analysis of EphB2 and ephrin-B1 protein levels in Caco-2 cells. The protein expression was normalized to β-actin. (B) Western blotting analysis of RhoA, ROCK1 and ROCK2 proteins and quantitative analysis of RhoA, ROCK1 and ROCK2 protein levels in Caco-2 cells.The protein expression was normalized to β-actin. Statistical analysis performed using one-way ANOVA with a Tukey Kramer post-hoc test. **P* 0.05, ***P* 0.01, ****P* 0.001, *****P* 0.0001.

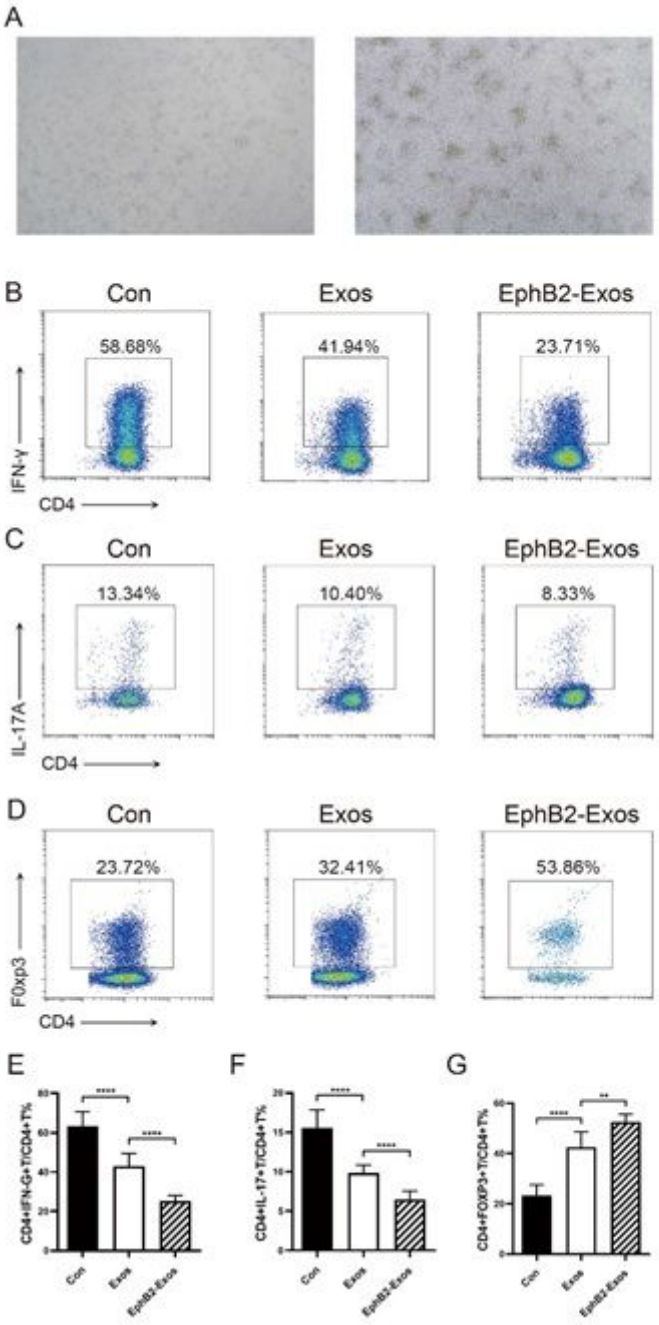

Figure 7

EphB2-Exos regulated CD4+ T cell polarization in vitro. (A) CD4+ T cells in the unstimulated state and after 72h stimulation of cytokines under optical microscope (Original magnification, × 40). Cell proliferation and colony growth after treatment. (B) The representative FACS plots of CD4+IFN-γ+Th1 cells.(C) The representative FACS plots of CD4+IL-17A+Th17 cells.(D) The representative FACS plots of CD4+Foxp3+Treg cells.(E) The average frequencies of Th1, Th17 and Treg cells in CD4+ T cells. Statistical analysis performed using one-way ANOVA with a Tukey Kramer post-hoc test. ***P* 0.01, *****P* 0.0001.

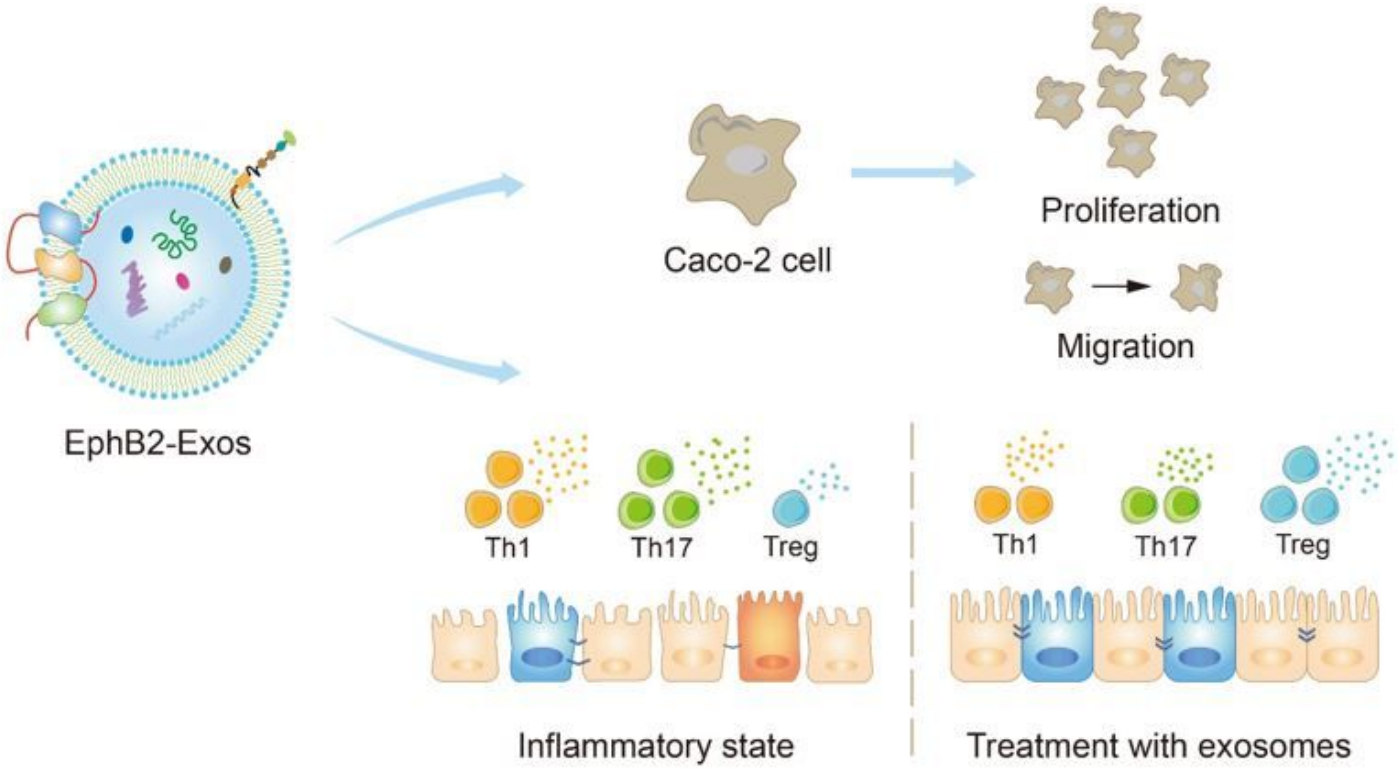

Figure 8

Schematic diagram of EphB2-Exos enhancing Caco-2 cells function and regulating the polarization of CD4+ T cells.

Supplementary Files

This is a list of supplementary files associated with this preprint. Click to download.

- NTA.wmv